

Exhaustive investigation of the duration of inflation in effective anisotropic loop quantum cosmology

Linda Linsefors*

*Laboratoire de Physique Subatomique et de Cosmologie, UJF, INPG, CNRS, IN2P3
53, avenue des Martyrs, 38026 Grenoble cedex, France*

Aurelien Barrau†

*Laboratoire de Physique Subatomique et de Cosmologie, UJF, INPG, CNRS, IN2P3
53, avenue des Martyrs, 38026 Grenoble cedex, France*

(Dated: March 16, 2019)

This article addresses the issue of estimating the duration in inflation in bouncing cosmology when anisotropies, inevitably playing an important role, are taken into account. It is shown that in Bianchi-I loop quantum cosmology, the higher the shear, the shorter the period of inflation. For a wide range of parameters, the probability distribution function of the duration of inflation is however peaked at values compatible with data, but not much higher. This makes the whole bounce/inflationary scenario consistent and phenomenologically appealing as all the information from the bounce might then not have been fully washed out.

I. INTRODUCTION

Loop quantum gravity (LQG) is an attempt of deriving a background-independent and non-perturbative quantization of general relativity. In the canonical formalism, it relies on Ashtekar variables, namely $SU(2)$ valued connections and conjugate densitized triads. The quantization is basically obtained through holonomies of the connections and fluxes of the densitized triads. Quite a lot of impressive results were recently obtained including an extensive covariant reformulation (see, *e.g.*, [1] for introductions and reviews).

Loop quantum cosmology (LQC) tries to capture the main features of LQG in the highly symmetric situations relevant for cosmology. A generic and important result of LQC is that the big bang is replaced by a big bounce due to strong repulsive quantum geometrical effects (see, *e.g.*, [2] for reviews and [3] for a recent numerical test of the bounce robustness).

In all bouncing cosmologies (except ekpyrotic models build to avoid this problem), either from the loop approach or any other, the issue of anisotropies is crucial for a very clear reason: the shear term basically varies as $1/a^6$ where a is the "mean" scale factor of the Universe. When the Universe is contracting, the shear term becomes more and more important and might drive the dynamics. The very reason why the shear can be safely neglected in standard cosmology is precisely the reason why it becomes essential in bouncing models. When one assumes spatial homogeneity, anisotropic hypersurfaces admit transitive groups of motion that must be three- or four-parameters isometry groups. The four-parameters groups having no simply transitive

subgroups, they will not be considered here. There are nine algebraically inequivalent three-parameters simply transitive Lie groups: Bianchi I through IX, all with well known structure constants. The flat, closed and open generalizations of the FLRW model are respectively called Bianchi-I, Bianchi-IX and Bianchi-V. In the following, we focus on the Bianchi-I model to study the dynamics around the bounce as the Universe is nearly flat today and as the relative weight of the curvature term in the Friedmann equation is decreasing with increasing values of the density.

Different studies have already been devoted to Bianchi-I LQC [4, 5]. In particular, it was shown that the bounce prediction resists the introduction of anisotropies. As the main features of isotropic LQC are well captured by semi-classical effective equations [3], we will assume that this remains true when anisotropies are included. The solutions of effective equations were studied in [6]. In a previous work, we have systematically explored the full solution space in a way that has not been considered before and have derived the LQC-modified generalized Friedmann equation that was still missing [7]. In another work, we established that, if initial conditions are set in the contracting phase, the duration of inflation is not anymore a free parameter but becomes a highly peaked distribution in isotropic effective LQC [8]. In this article, we address both questions at the same time: how is the duration of inflation affected by anisotropies that *must* be taken into account in any consistent bouncing approach?

II. GRAVITATIONAL SECTOR

We refer the reader to [7] for detailed notations. The metric for a Bianchi-I spacetime is given by

$$ds := -N^2 d\tau^2 + a_1^2 dx^2 + a_2^2 dy^2 + a_3^2 dz^2, \quad (1)$$

* linsefors@lpsc.in2p3.fr

† Aurelien.Barrau@cern.ch

where a_i denote the directional scale factors. The classical gravitational hamiltonian is

$$\mathcal{H}_G = \frac{N}{\kappa\gamma^2} \left(\sqrt{\frac{p_1 p_2}{p_3}} c_1 c_2 + \sqrt{\frac{p_2 p_3}{p_1}} c_2 c_3 + \sqrt{\frac{p_3 p_1}{p_2}} c_3 c_1 \right), \quad (2)$$

with Poisson brackets

$$\{c_i, p_j\} = \kappa\gamma\delta_{ij}. \quad (3)$$

The classical directional scale factors can be written as

$$a_1 = \sqrt{\frac{p_2 p_3}{p_1}} \quad \text{and cyclic expressions.} \quad (4)$$

The generalized Friedmann equation is

$$H^2 = \sigma^2 + \frac{\kappa}{3}\rho, \quad (5)$$

where

$$H := \frac{\dot{a}}{a} = \frac{1}{3}(H_1 + H_2 + H_3), \quad a := (a_1 a_2 a_3)^{1/3}, \quad (6)$$

$$H_1 := \frac{\dot{a}_1}{a_1} = -\frac{\dot{p}_1}{2p_1} + \frac{\dot{p}_3}{2p_3} + \frac{\dot{p}_2}{2p_2} \quad \text{and cyclic expressions.} \quad (7)$$

The holonomy correction now has to be implemented to account for specific loop quantum gravity effects. It is rooted in the fact that the Ashtekar connection cannot be promoted to be an operator whereas its holonomy can. It is assumed to captures relevant quantum effects at the semi-classical level. Following the usual prescription, one substitutes

$$c_i \rightarrow \frac{\sin(\bar{\mu}_i c_i)}{\bar{\mu}_i} \quad (8)$$

in the classical Hamiltonian. The $\bar{\mu}_i$ are given by

$$\bar{\mu}_1 = \lambda \sqrt{\frac{p_1}{p_2 p_3}} \quad \text{and cyclic expressions,} \quad (9)$$

where λ is the square root of the minimum area eigenvalue of the LQG area operator ($\lambda = \sqrt{\Delta}$), originally derived in [4]. The quantum corrected gravitational Hamiltonian is:

$$\mathcal{H}_G = -\frac{N\sqrt{p_1 p_2 p_3}}{\kappa\gamma^2\lambda^2} \left[\sin(\bar{\mu}_1 c_1) \sin(\bar{\mu}_2 c_2) + \sin(\bar{\mu}_2 c_2) \sin(\bar{\mu}_3 c_3) + \sin(\bar{\mu}_3 c_3) \sin(\bar{\mu}_1 c_1) \right]. \quad (10)$$

In the gravitational sector, all the information is contained in the h_i :

$$h_1 := \bar{\mu}_1 c_1 = \lambda \sqrt{\frac{p_1}{p_2 p_3}} c_1 \quad \text{and cyclic expressions.} \quad (11)$$

The six gravitational degrees of freedom (c_i, p_i) account for only three physical degrees of freedom h_i .

The observable quantities for the gravitational field can be described by h_1, h_2, h_3 and there equations of motion[7]:

$$\dot{h}_1 = \frac{1}{2\gamma\lambda} \left[(h_2 - h_1)(\sin h_1 + \sin h_3) \cos h_2 + (h_3 - h_1)(\sin h_1 + \sin h_2) \cos h_3 \right] - \frac{\kappa\gamma\lambda}{2}(\rho + P) \quad \text{and cyclic expressions,} \quad (12)$$

where ρ is the total matter energy density and P is the total pressure of matter.

From h_1, h_2 and h_3 , we can get the directional Hubble parameters

$$H_1 := \frac{\dot{a}_1}{a_1} = \frac{1}{2\gamma\lambda} \left[\sin(h_1 - h_2) + \sin(h_1 - h_3) + \sin(h_2 + h_3) \right] \quad \text{and cyclic expressions,} \quad (13)$$

and the average Hubble parameter

$$H := \frac{\dot{a}}{a} = \frac{1}{3}(H_1 + H_2 + H_3) = \frac{1}{6\gamma\lambda} \left[\sin(h_1 + h_2) + \sin(h_2 + h_3) + \sin(h_3 + h_1) \right]. \quad (14)$$

By defining the quantum shear:

$$\sigma_Q^2 := \frac{1}{3\gamma^2\lambda^2} \left(1 - \frac{1}{3} \left[\cos(h_1 - h_2) + \cos(h_2 - h_3) + \cos(h_3 - h_1) \right] \right), \quad (15)$$

one can write down the LQC-modified generalized Fried-

man equation:

$$H^2 = \sigma_Q^2 + \frac{\kappa}{3}\rho - \lambda^2\gamma^2 \left(\frac{3}{2}\sigma_Q^2 + \frac{\kappa}{3}\rho \right)^2. \quad (16)$$

When σ_Q^2 is small in plank units, it can be approximated by $\sigma_Q^2 \approx \frac{1}{18}[(H_1 - H_2)^2 + (H_2 - H_3)^2 + (H_3 - H_1)^2]$, which is the classical shear, up to a constant.

From Eqs. (12) and (14), we find that

$$(\dot{h}_i - \dot{h}_j) = -3H(h_i - h_j), \quad (17)$$

and from this, it follows that

$$(h_i - h_j) \propto a^{-3}. \quad (18)$$

Without loss of generality, one can choose the labeling of the spacial dimensions such that initially

$$h_1 \leq h_2 \leq h_3. \quad (19)$$

Because of Eq. (18), we know that this inequality will hold at any time.

We now define a the symmetry measure for the anisotropy

$$S := \frac{(h_2 - h_1) - (h_3 - h_2)}{(h_3 - h_1)}. \quad (20)$$

It follows from Eq. (18), that S is a constant of motion, and it follows from its definition and Eq. (19) that $-1 \leq S \leq 1$.

III. MATTER

A matter field has to be introduced. It will of course play a crucial role in the inflationary phase. We will choose a simple massive scalar field with potential

$$V(\phi) = \frac{m^2 \phi^2}{2}. \quad (21)$$

This is the simplest potential that will generate slow roll inflation, and therefore a good generic toy model. In addition, this potential, that was somehow slightly disfavored by Planck data, is now favored again by the new results from BICEP2 [11].

Given this potential, the equation of motion for the scalar field is:

$$\ddot{\phi} = -3H\dot{\phi} - m^2\phi. \quad (22)$$

The above equation, together with Eqs. (12), is the full set of equations of motion describing the system under study in this work.

IV. SIMULATIONS

We have performed exhaustive numerical simulations (with control of the numerical errors) to investigate the duration of inflation as a function of the different variables entering the dynamics. All the simulations

carried out is this work are started in the contracting phase, with small energy density and shear, so that everything is well described by unmodified classical equations. In addition, all the simulations start with $\sigma_Q^2 \ll \frac{\kappa}{3}\rho$. For all solutions that have a classical past at all¹, $\sigma_Q^2 \ll \frac{\kappa}{3}\rho$ will be fulfilled at some early enough time.

Since the shear is initially small compared to everything else, we will choose the initial conditions for the matter content in the same way as in [8]:

$$\rho(0) = \rho_0 \left(1 - \frac{1}{2} \sqrt{3\kappa\rho_0} \frac{1}{2m} \sin(2\delta)\right)^{-2}, \quad (23)$$

$$m\phi(0) = \sqrt{2\rho(0)} \sin(\delta), \quad (24)$$

and

$$\dot{\phi}(0) = \sqrt{2\rho(0)} \cos(\delta), \quad (25)$$

where ρ_0 is the initial energy density up to a small correction, and δ is the phase of the oscillations between the kinetic and the potential energy. As demonstrated in [8], it is a natural variable for which one can assume a flat probability distribution function. It is of course not anymore the only unknown "random" variable when the shear is included.

Since everything is initially very small in Plank units, we can approximate:

$$H(0) \approx \frac{3}{3\gamma\lambda} [h_1(0) + h_2(0) + h_3(0)], \quad (26)$$

$$\sigma_Q^2(0) \approx \frac{1}{18\gamma^2\lambda^2} \left[(h_1(0) - h_2(0))^2 + (h_2(0) - h_3(0))^2 + (h_3(0) - h_1(0))^2 \right]. \quad (27)$$

Solving the above equations together with Eq. (20) gives for $h_1(0)$, $h_2(0)$ and $h_3(0)$:

$$h_1(0) \approx \gamma\lambda H(0) + \gamma\lambda \frac{-3 - S}{\sqrt{3 + S^2}} \sqrt{\sigma_Q^2(0)}, \quad (28)$$

$$h_2(0) \approx \gamma\lambda H(0) + \gamma\lambda \frac{2S}{\sqrt{3 + S^2}} \sqrt{\sigma_Q^2(0)}, \quad (29)$$

$$h_3(0) \approx \gamma\lambda H(0) + \gamma\lambda \frac{3 - S}{\sqrt{3 + S^2}} \sqrt{\sigma_Q^2(0)}. \quad (30)$$

¹ Many solutions to the equations we use will never approach the classical behavior [7]. In this article we avoid these solutions by choosing initial conditions within the classical regime. A contracting universe that starts out close to the classical limit, will always approach the classical limit again after the bounce.

Finally, the initial conditions have to fulfill Eq. (16), and since we are in the contracting branch we get the negative solution for $H(0)$,

$$H(0) = -\sqrt{\sigma_Q^2(0) + \frac{\kappa}{3}\rho(0) - \lambda^2\gamma^2 \left(\frac{3}{2}\sigma_Q^2(0) + \frac{\kappa}{3}\rho(0)\right)^2}. \quad (31)$$

The initial conditions of the simulations are specified by Eqs. (23)-(25) and (28)-(31), and the parameters ρ_0 , δ , $\sigma_Q^2(0)$ and S .

To make sure that the approximations used for the initial conditions hold, the parameters must fulfill:

$$\sigma_Q^2(0) \ll \frac{\kappa}{3}\rho_0 \ll m^2, \quad (32)$$

together with, from the definitions:

$$-1 \leq S \leq 1 \quad \text{and} \quad 0 \leq \delta < 2\pi. \quad (33)$$

For all the simulations in this work, we have used $m = 1.21 \times 10^{-6}$, as favored by observation [12]. In addition, we have used $\frac{\kappa}{3}\rho_0 = 10^{-3}m^2$, and $\sigma_Q^2(0) \in [0, 10^{-5}m^2]$.

V. RESULTS

We are interested in investigating how anisotropies affect the length of slow-roll inflation. The number of e-folds of inflation, N , can be calculated from the value of the scalar field at the beginning of the slow-roll phase ϕ_{infl} :

$$N = 2\pi\phi_{infl}^2. \quad (34)$$

The simulations confirm that the slow-roll inflation starts when $|\phi|$ reaches its maximum value after the bounce.

A. Symmetry

Classically (*i.e.* with no quantum corrections), the value of S does not influence the evolution at all. In the effective LQC case, S does influence the shape of the bounce. This can be seen in Fig. 1. However, we are interested in how S affects slow-roll inflation.

In Fig. 2, is shown the resulting ϕ_{infl} , as an output of simulations, with varying S . The results are basically flat. We conclude that the symmetry affects some details of the shape of the bounce, but has no effect on the duration of slow-roll inflation. Therefore, $S = 0$ is chosen for the rest of this study.

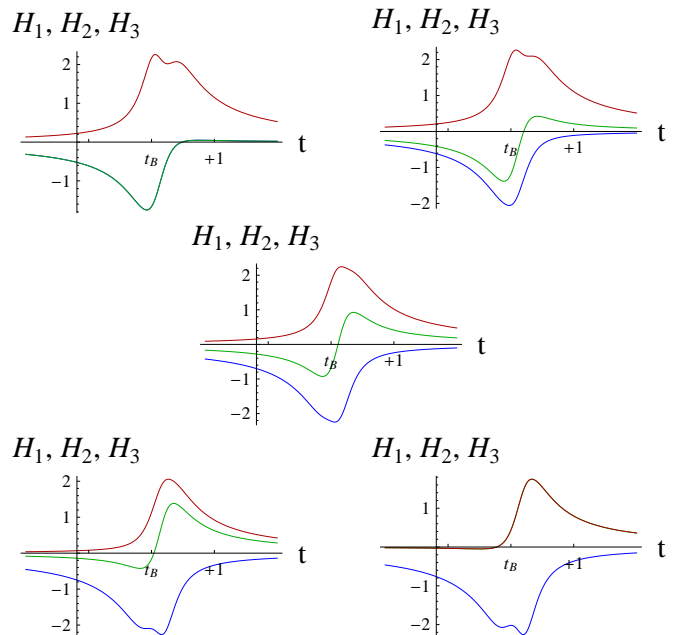


FIG. 1. Details of the bounce showed for different values of the symmetry factor S . Upper left: $S = -1$. Upper right: $S = -0.5$. Center: $S = 0$. Lower left: $S = 0.5$. Lower right: $S = 1$. Red is H_3 , green is H_2 and blue is H_1 . $\sigma_Q^2(0) = 10^{-2}\frac{\kappa}{3}\rho_0$ and $\delta = 0$ for all the above plots.

B. Shear

In this section we vary $\sigma_Q^2(0)$ and δ to see how this affects the length of slow-roll inflation.

The result of extensive simulations are showed in Fig. 5. It can be concluded that, in general, the number of e-folds goes down when the shear increases. But a greater shear will also lead to a bigger spread in the number of e-folds, depending on the initial angle δ .

In Fig. 3, one can see that the number of e-folds of slow-roll inflation depends strongly on ρ_{max} , which is of course not surprising. When the shear vanishes, ρ_{max} becomes fixed, otherwise it can vary between zero and the associated maximum value.

At the bounce, the universe is completely dominated by the kinetic energy and the shear. The kinetic energy grows a lot during a very short time. This gives the scalar field a boost, and lifts it up to create the initial conditions for slow-roll inflation. If there is a lot of shear, the bounce will happen at a lower value of the kinetic energy, and the scalar field potential will not be lifted as high as in the isotropic case. Fig. 4 shows a typical behavior of the field around the bounce.

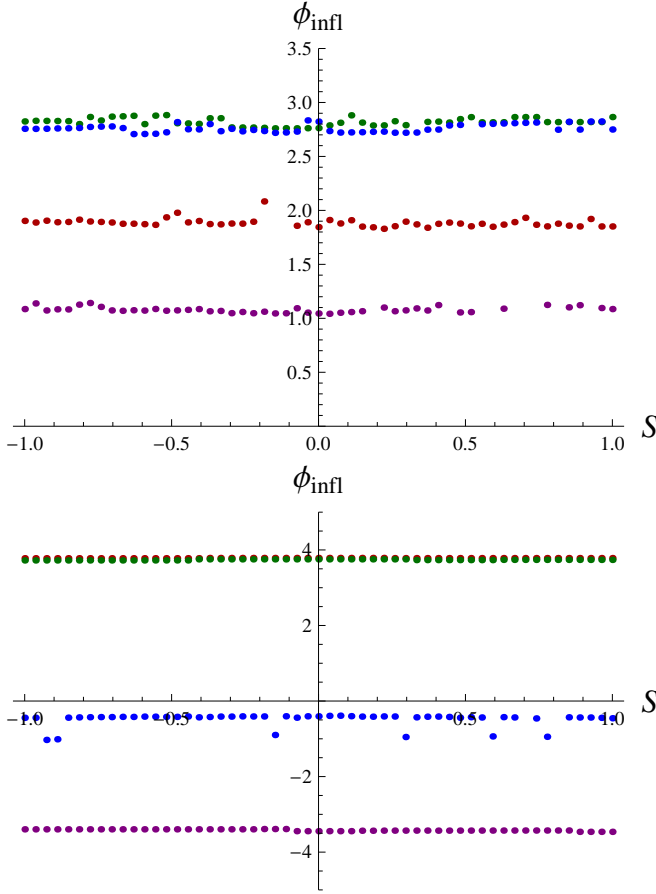


FIG. 2. Scalar field at the beginning of inflation as a function of S . Upper: $\sigma_Q^2(0) = 10^{-2} \frac{\kappa}{3} \rho_0$. Lower: $\sigma_Q^2(0) = 10^{-3} \frac{\kappa}{3} \rho_0$. Red is $\delta = 0$, green is $\delta = \frac{\pi}{4}$, blue is $\delta = \frac{\pi}{2}$ and purple is $\delta = \frac{3\pi}{4}$. Note that in the lower plot, the green points are right on top of the red ones and are therefore hard to be seen.

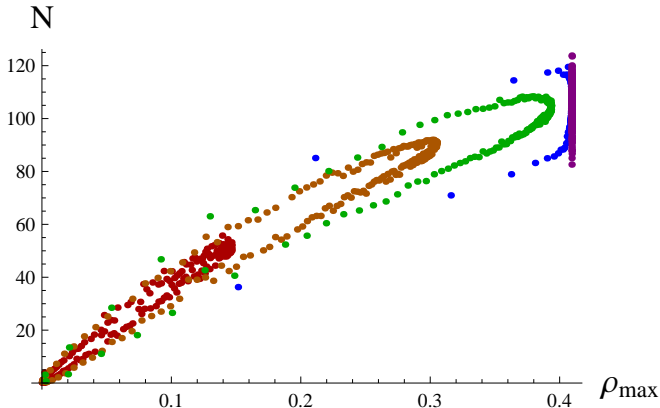


FIG. 3. Number of e-folds as a function of ρ at the bounce. Red: $\sigma_Q^2(0) = 10^{-2} \frac{\kappa}{3} \rho_0$. Orange: $\sigma_Q^2(0) = 10^{-3} \frac{\kappa}{3} \rho_0$. Green: $\sigma_Q^2(0) = 10^{-4} \frac{\kappa}{3} \rho_0$. Blue: $\sigma_Q^2(0) = 10^{-6} \frac{\kappa}{3} \rho_0$. Purple: $\sigma_Q^2(0) = 0$.

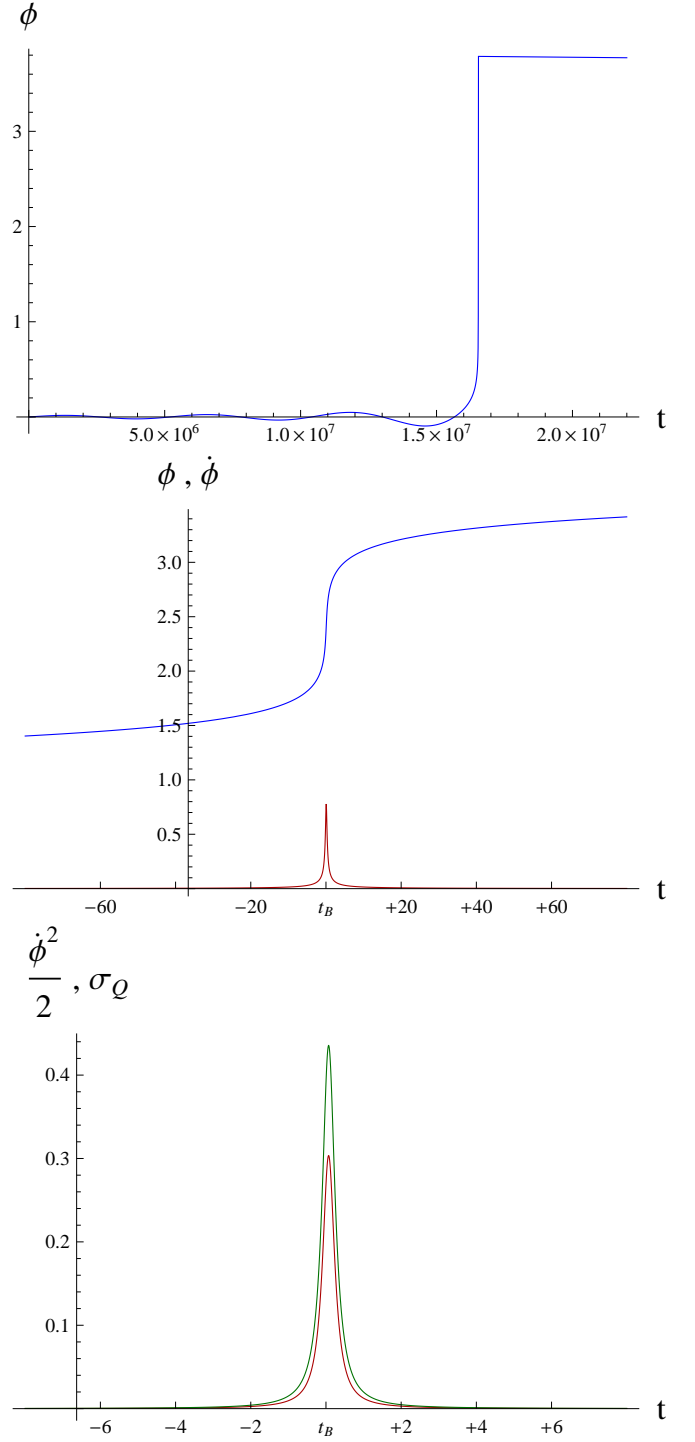


FIG. 4. Typical evolution of ϕ , $\dot{\phi}$, and σ_Q^2 as a function of time. The blue line is ϕ , the red is $\dot{\phi}$ or $\frac{\dot{\phi}^2}{2}$, and the green is σ_Q^2 . All the above plots are from the same simulation. Note that the kinetic energy is always completely dominating over the potential energy at the bounce $\frac{\dot{\phi}^2}{2} \gg \frac{m^2 \phi_B^2}{2}$. The fraction of shear and potential energy at the bounce varies, depending on the initial conditions. The initial conditions are $\sigma_Q^2(0) = 10^{-3} \frac{\kappa}{3} \rho_0$, $S = 0$ and $\delta = 0$.

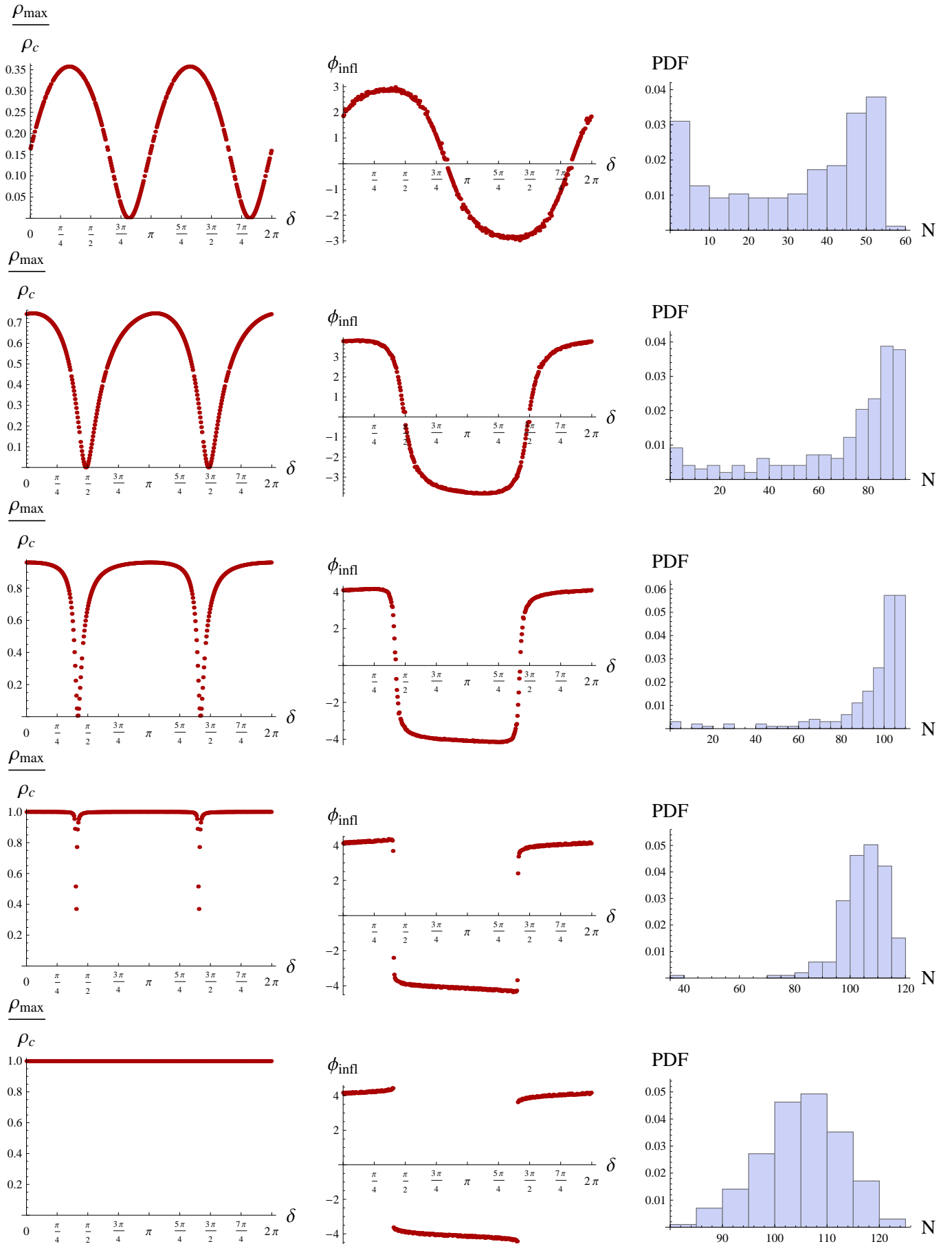


FIG. 5. Results of the simulations, for each row, starting from the top $\sigma_Q^2(0) = \{10^{-2} \frac{\kappa}{3} \rho_0, 10^{-3} \frac{\kappa}{3} \rho_0, 10^{-4} \frac{\kappa}{3} \rho_0, 10^{-6} \frac{\kappa}{3} \rho_0, 0\}$. First column: The maximum value of ρ (which is the value of ρ at the bounce), divided by ρ_c . Second column: ϕ at the start of slow-roll inflation. Third column: Numerically calculated probability distribution function of the number of e-folds of slow-roll inflation, given that all δ have equal probability.

VI. CONCLUSIONS

This article takes into account anisotropies to investigate exhaustively the expected duration of inflation in effective loop quantum cosmology. Basically, anisotropies lead to a lower energy density at the bounce, which leads to fewer e-folds of slow-roll inflation. It is however quite impressive that for a wide range of parameters, say for $\sigma_Q^2(0) < 5 \times 10^{-3} \frac{\kappa}{3} \rho_0$, the probability distribution function for the number of e-folds is peaked at values compatible with data, between 70 and 110 e-

folds². It is remarkable that whereas any value between 0 and $N_{max} = 2\pi\sqrt{2\rho_c}m^{-2} = 3.9 \times 10^{12}$ is *a priori* possible for N , the result is so close to the minimum required value. This makes the bounce/inflation scenario particularly appealing and possibly important for phenomenology: all the quantum information from the bounce might not have been fully washed out by inflation. Having N close to 70 is exactly what is required to lead to measurable effects in the CMB spectrum. An important point however remains unanswered: what would be a "natural" initial value for the shear?

-
- [1] P. Dona & S. Speziale, arXiv:1007.0402V1;
 A. Perez, arXiv:gr-qc/0409061v3;
 R. Gambini & J. Pullin, *A First Course in Loop Quantum Gravity*, Oxford, Oxford University Press, 2011;
 C. Rovelli, arXiv:1102.3660v5 [gr-qc];
 C. Rovelli, *Quantum Gravity*, Cambridge, Cambridge University Press, 2004;
 C. Rovelli, *Living Rev. Relativity*, 1, 1, 1998;
 L. Smolin, arXiv:hep-th/0408048v3;
 T. Thiemann, *Lect. Notes Phys.*, 631, 41, 2003; T. Thiemann, *Modern Canonical Quantum General Relativity*, Cambridge, Cambridge University Press, 2007
- [2] A. Ashtekar, M. Bojowald, and J. Lewandowski, *Adv. Theor. Math. Phys.* 7, 233, 2003;
 A. Ashtekar, *Gen. Rel. Grav.* 41, 707, 2009;
 A. Ashtekar, P. Singh, *Class. Quantum Grav.* 28, 213001, 2011;
 M. Bojowald, *Living Rev. Rel.* 11, 4, 2008;
 M. Bojowald, arXiv:1209.3403 [gr-qc];
 K. Banerjee, G. Calcagni, and M. Martin-Benito, *SIGMA* 8, 016, 2012;
 G. Calcagni, *Ann. Phys. (Berlin)* 525, 323, 2013;
 I. Agullo and A. Corichi, in "The Springer Handbook of Spacetime," edited by A. Ashtekar and V. Petkov. (Springer-Verlag, at Press); arXiv:1302.3833 [gr-qc];
 A. Barrau *et al.*, *Class. Quant. Grav.* 31, 053001, 2014
- [3] P. Diener, B. Gupt, P. Singh, arXiv:1402.6613
- [4] A. Ashtekar, E. Wilson-Ewing, *Phys. Rev. D* 79, 083535, 2009
- [5] D. Cartin, G. Khanna, *Phys. Rev. Lett.* 94, 111302, 2005;
 G. Date, *Phys. Rev. D* 72, 067301, 2005;
 D. Cartin, G. Khanna, *Phys. Rev. D* 72, 084008, 2005;
 D.-W. Chiou, *Phys. Rev. D* 75, 024029, 2007;
 D.-W. Chiou, arXiv:gr-qc/0703010;
 D.-W. Chiou, Kevin Vandersloot, *Phys. Rev. D*, 76, 084015, 2007;
- D.-W. Chiou, *Phys. Rev. D* 76, 124037, 2007;
 L. Szulc, *Phys. Rev. D* 78, 064035, 2008;
 M. Martin-Benito, G.A. Mena Marugan, T. Pawłowski, *Phys. Rev. D* 78, 064008, 2008;
 D.-W. Chiou, arXiv:0812.0921 [gr-qc];
 P. Dzierzak, W. Piechocki, *Phys. Rev. D* 80, 124033, 2009;
 M. Martin-Benito, G. A.Mena Marugan, Tomasz Pawłowski, *Phys. Rev. D* 80, 084038, 2009;
 P. Dzierzak, W. Piechocki, *Annalen Phys.* 19, 290, 2012;
 P. Malkiewicz, W. Piechocki, P. Dzierzak, *Class. Quant. Grav.* 28, 085020, 2011;
 M. Martin-Benito, L.J. Garay, G.A. Mena Marugan, E. Wilson-Ewing, *J. Phys. Conf. Ser.* 360, 012031, 2012;
 V. Rikhvitsky, B. Saha, M. Visinescu, *Astrophys. Space Sci.* 339, 371, 2012;
 P. Singh, *Phys. Rev. D* 85, 104011, 2012;
 F. Cianfrani, A. Marchini, G. Montani, *Europhys. Lett.* 99, 10003, 2012;
 K. Fujio, T. Futamase, *Phys. Rev. D* 85, 124002, 2012;
 P. Singh, *J. Phys. Conf. Ser.* 360, 012008, 2012;
 X. Liu, F. Huang, J.-Y. Zhu, *Class. Quant. Grav.* 30, 065010, 2013;
 X.-J. Yue, J.-Y. Zhu, arXiv:1302.1014 [gr-qc]
- [6] B. Gupt and P. Singh, arXiv:1304.7686 [gr-qc]
- [7] L. Linsefors and A. Barrau, *Class. Quant. Grav.* 31, 015018, 2014 [arXiv:1305.4516 [gr-qc]].
- [8] L. Linsefors and A. Barrau, *Phys. Rev. D* 87, 123509, 2013
- [9] K.C. Jacobs, "Bianchi I cosmological models", PhD thesis, Caltech, 1969
- [10] A. Ashtekar and D. Sloan, *Phys. Lett. B*, 694, 108, 2012;
 A. Ashtekar and D. Sloan, *Gen. Rel. Grav.*, 43, 3519, 2011
- [11] P. A. R. Ade *et al.* [BICEP2 Collaboration], arXiv:1403.3985 [astro-ph.CO].
- [12] A. Linde, arXiv:1402.0526

² Even without shear, the distribution obtained here is not exactly the same as in [8], due to details in the way the simulations are

carried out. This does not affect the overall conclusions.